

Photoluminescence properties of erbium doped InGaN epilayers

A. Sedhain,^{1,2} C. Ugolini,² J. Y. Lin,¹ H. X. Jiang,^{1,a)} and J. M. Zavada³

¹Department of Electrical and Computer Engineering, Texas Tech University, Lubbock, Texas 79409, USA

²Department of Physics, Kansas State University, Manhattan, Kansas 66506, USA

³Department of Electrical and Computer Engineering, North Carolina State University, Raleigh, North Carolina 27695-7911, USA

(Received 7 June 2009; accepted 9 July 2009; published online 30 July 2009)

We report on the photoluminescence properties of erbium (Er) doped $\text{In}_x\text{Ga}_{1-x}\text{N}$ epilayers synthesized by metal organic chemical vapor deposition. The crystalline quality and surface morphology of Er doped $\text{In}_{0.05}\text{Ga}_{0.95}\text{N}$ were nearly identical to those of Er doped GaN. The photoluminescence intensity of the 1.54 μm emission in Er doped $\text{In}_{0.05}\text{Ga}_{0.95}\text{N}$ was an order of magnitude lower than in Er doped GaN and decreased with the increase of the In content. The reduction in 1.54 μm emission intensity was accompanied by enhanced emission intensities of deep level impurity transition lines. © 2009 American Institute of Physics. [DOI: 10.1063/1.3193532]

Due to the outstanding physical properties of III-nitride wide bandgap semiconductors, the possibility of using GaN as a host medium for erbium (Er) doping for optical communication applications has been explored.¹⁻⁹ Recently, we have shown that Er doped GaN epilayers grown by metal organic chemical vapor deposition (MOCVD) possess a high Er concentration and exhibit a strong photoluminescence (PL) emission at 1.54 μm with a low degree of thermal quenching ($\sim 20\%$ between 10 and 300 K).⁹ We have also shown that above bandgap excitation is much more efficient than below bandgap excitation for the Er emission at 1.54 μm ,¹⁰ suggesting that 1.54 μm optical devices based on Er doped GaN would be much more energy efficient operating in an above bandgap excitation scheme. On the other hand, high power III-nitride light emitting diodes (LEDs) and laser diodes (LDs) operating at wavelengths between 370–540 nm are commercially available, which could conveniently facilitate an above bandgap excitation scheme at the chip level if the active medium were based on Er doped InGaN rather than Er doped GaN. However, the growth of Er-doped InGaN epilayers with an efficient 1.54 μm emission has not been achieved. In this work, we investigate the optical and structural properties of Er doped InGaN synthesized by MOCVD.

The Er doped InGaN sample structure used for this work was very similar to the previously studied Er doped GaN.⁹ The growth of the epilayer began with a thin GaN buffer layer and a 1.2 μm GaN epi-template followed by a 300 nm Er doped InGaN layer grown at 760 °C. The In content of the Er doped InGaN epilayers was determined by the x-ray diffraction (XRD) peak positions of θ -2 θ scans of the (002) plane. The full width at half maximum (FWHM) of rocking curves of the (002) diffraction peaks were utilized to determine the crystalline quality and the optical properties were determined using the same PL system used for Er doped GaN.⁹

Figure 1 is a θ -2 θ XRD scan for Er doped InGaN grown in the same growth conditions (Er and NH_3 flow rates, etc.) as Er doped GaN but at a lower growth temperature of 760 °C (versus 1040 °C for Er doped GaN). Clear peaks are

observed at 34.36° and 34.52° corresponding to the (002) diffraction peaks of $\text{In}_{0.05}\text{Ga}_{0.95}\text{N}$ and GaN, respectively. The inset of Fig. 1 contains a comparison of the (002) XRD rocking curves of Er doped $\text{In}_{0.05}\text{Ga}_{0.95}\text{N}$ and GaN, which reveals that the crystalline quality of Er doped InGaN is nearly identical to that of Er doped GaN. The root mean square (rms) surface roughness of Er doped $\text{In}_{0.05}\text{Ga}_{0.95}\text{N}$ is higher (4 nm) than that of Er doped GaN (2 nm). The concentration of Er in InGaN:Er is comparable to that in GaN:Er ($\sim 10^{21}/\text{cm}^3$), as determined by secondary ion mass spectroscopy measurements by Evan's analytical group. Figure 2 compares the room temperature (300 K) PL spectra of Er doped (a) $\text{In}_{0.05}\text{Ga}_{0.95}\text{N}$ and (b) GaN for an excitation laser wavelength set at 263 nm. It is noted that the 1.54 μm emission intensity from $\text{In}_{0.05}\text{Ga}_{0.95}\text{N}$:Er is almost an order of magnitude lower

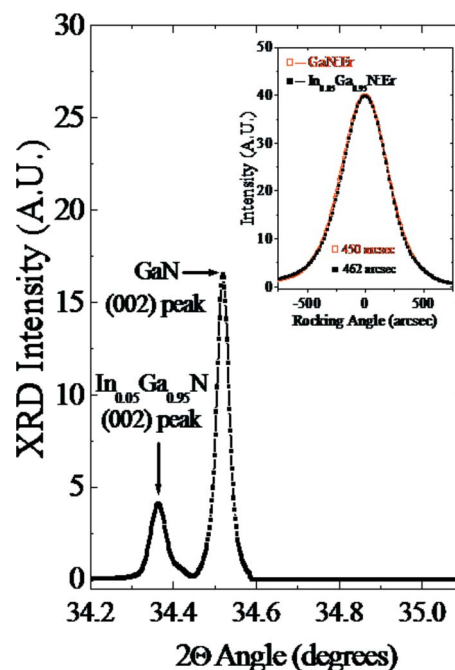


FIG. 1. (Color online) θ -2 θ XRD scan of the (002) peak of Er doped $\text{In}_{0.05}\text{Ga}_{0.95}\text{N}$ grown on GaN/sapphire template. The insert shows the XRD rocking curves of the (002) peak of Er doped GaN and Er doped $\text{In}_{0.05}\text{Ga}_{0.95}\text{N}$. The numbers located under the curves indicate the FWHM of the rocking curves.

^{a)}Electronic mail: hx.jiang@ttu.edu.

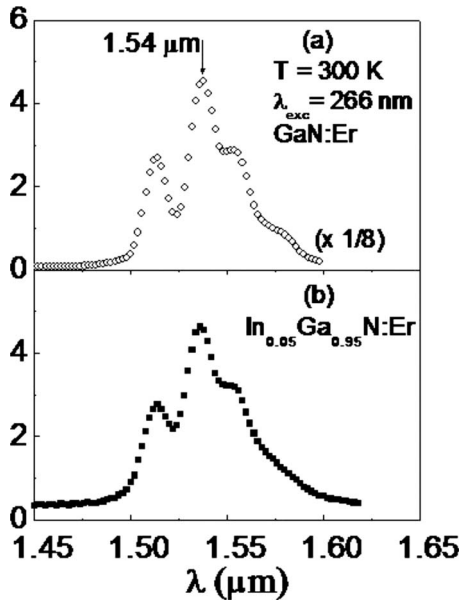


FIG. 2. PL spectra of Er doped GaN and Er doped $\text{In}_{0.05}\text{Ga}_{0.95}\text{N}$ measured at 300 K for an excitation wavelength (λ_{exc}) of 263 nm.

than that from GaN:Er, despite the fact that both epilayers have a comparable crystalline quality, surface morphology, and Er concentration.

Er doped InGaN epilayers grown with varying growth pressures, NH_3 , and Ga flow rates were investigated in an attempt to increase the In fraction and optimize the emission at $1.54 \mu\text{m}$. Their low temperature PL emission properties in both the $1.54 \mu\text{m}$ window and visible spectral region have been studied to explore possible mechanisms responsible for the drastic drop in the $1.54 \mu\text{m}$ emission intensity in InGaN:Er. Figure 3 shows that the ratio of the $1.54 \mu\text{m}$ emission intensity from GaN:Er to that from $\text{In}_{0.05}\text{Ga}_{0.95}\text{N}$:Er is about 5 at 10 K, which implies that the thermal quenching of the $1.54 \mu\text{m}$ emission is more severe in $\text{In}_{0.05}\text{Ga}_{0.95}\text{N}$:Er than in GaN:Er, which is expected for a lower band-gap material.² The results shown in Fig. 3 also clearly reveal that an increase in In content is accompanied with a rapid reduction of the emission intensity at $1.54 \mu\text{m}$ and concomitantly, new emission bands emerge in the visible spectral region. In a sharp contrast to the case of GaN:Er in which only a weak band-edge emission line at 3.21 eV is observable,¹¹ three strong emission lines emerge in $\text{In}_{0.05}\text{Ga}_{0.95}\text{N}$:Er. Red and yellow bands centered around

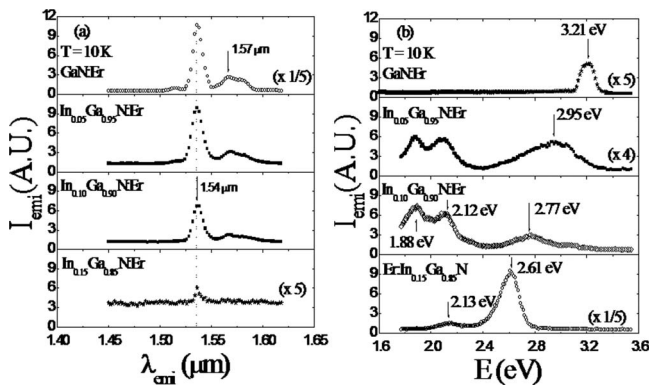


FIG. 3. Low temperature (10 K) PL spectra of GaN:Er and InGaN:Er in (a) $1.54 \mu\text{m}$ and (b) visible spectral region.

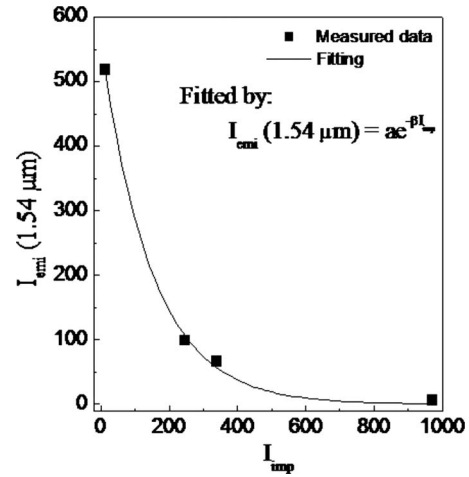


FIG. 4. PL peak emission intensity at $1.54 \mu\text{m}$ as a function of integrated emission intensity of all observable impurity lines in the visible spectral region in InGaN:Er with different In contents. Solid line is the least-squares fit of data with Eq. (1).

1.86 and 2.10 eV were relatively weak and are observable in $\text{In}_x\text{Ga}_{1-x}\text{N}$:Er with lower x . A third emission peak at higher energy position (2.95, 2.77, and 2.61 eV for $x=0.05, 0.10,$ and 0.15 , respectively) becomes more prominent and exhibits a redshift with increasing In content.

Although the origins of these transitions are not yet fully understood, they are related to deep level impurities or impurity complexes (such as cation and anion vacancies and their complexes), based on their spectral peak positions. The correlation between the $1.5 \mu\text{m}$ emission and deep level impurity transitions is further revealed by plotting the emission intensity at $1.54 \mu\text{m}$ as a function of the visible emission intensity in InGaN:Er with different In contents. As illustrated in Fig. 4, the relationship is described by an exponential dependence:

$$I_{1.54 \mu\text{m}} = a e^{-\beta I_{\text{imp}}}, \tag{1}$$

where a and β are fitting parameters and I_{imp} denotes the integrated emission intensity of all observable impurity transition lines in the visible spectral region. The result shown in Fig. 4 clearly demonstrates that deep level impurity centers are more readily incorporated into InGaN:Er with higher In contents (or lower bandgaps), and that Er related emission intensities at $1.54 \mu\text{m}$ decrease exponentially with their concentration (or equivalently I_{imp}). The presence of deep level impurity centers in the host material offers alternative and efficient recombination routes in the visible spectral region and inhibits the energy transfer of photoexcited electrons and holes to the Er atoms. Thus, the presence of these impurities greatly diminishes the possibility of $4I_{13/2}-4I_{15/2}$ transition from Er and hence the emission intensity at $1.54 \mu\text{m}$.

Figure 5(a) is an Arrhenius plot of the integrated PL emission intensity of the $1.54 \mu\text{m}$ emission line from Er doped $\text{In}_{0.10}\text{Ga}_{0.90}\text{N}$ between 10 and 450 K based on the raw data shown in the inset. From this plot, energy of about 66 meV for the dominant thermal activation process was determined. Combining the temperature dependent PL data for GaN:Er and InGaN:Er, we have obtained the thermal activation energy (E_A) of the $1.54 \mu\text{m}$ emission line as a function of the bandgap energy of InGaN (or the In-content) and the

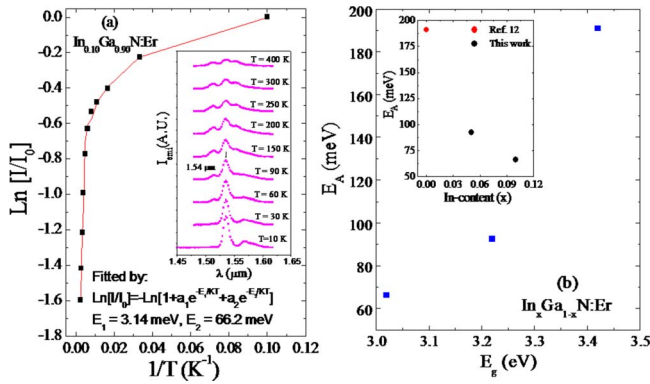


FIG. 5. (Color online) (a) Arrhenius plot of the integrated PL emission intensity of the $1.54 \mu\text{m}$ emission line from Er doped $\text{In}_{0.10}\text{Ga}_{0.90}\text{N}$ between 10 and 400 K based on the raw data shown in the inset. (b) The thermal activation energy (E_A) of the $1.54 \mu\text{m}$ emission line as a function of the bandgap energy of InGaN and the inset shows E_A as a function of the In-content in InGaN.

results are shown in Fig. 5(b), which clearly shows that E_A continuously decreases with a decrease of the energy bandgap of the InGaN host.

Compared to GaN:Er epilayers which were grown at 1040°C , the lower growth temperature of InGaN:Er (760°C) limited by a weaker bonding between In-N tends to generate more native defects such as nitrogen vacancies due to the insufficient decomposition of NH_3 . Furthermore, as the In content increases, the lattice mismatch between the InGaN:Er layer and the underlying GaN also increases, which results in more dislocations. More dislocations in general translate to more efficient impurity incorporation.

In summary, Er doped InGaN has been synthesized by MOCVD. The Er doped InGaN epilayer crystalline quality and surface morphology were comparable to those of Er

doped GaN, but the PL intensity of the $1.54 \mu\text{m}$ emission from Er doped InGaN was much lower than that from Er doped GaN. The drop in $1.54 \mu\text{m}$ emission intensity in Er doped InGaN was accompanied by enhanced visible emissions due to the presence of deep level impurities incorporated during the MOCVD growth of Er doped InGaN. The variable growth environments showed that increased In-content resulted in a lower Er emission intensity at $1.54 \mu\text{m}$, a trend that resembles the decrease of the efficiency of nitride LEDs as the emission wavelength varies from blue to green.

This work is supported by NSF under Grant No. (ECCS-0854619). H.X.J. and J.Y.L. would like to acknowledge the support of Edward Whitacre and Linda Whitacre endowment chair positions through the AT&T Foundation.

- ¹J. M. Zavada and D. Zhang, *Solid-State Electron.* **38**, 1285 (1995).
- ²P. N. Favenec, H. L'Haridon, M. Salvi, D. Moutonnet, and Y. LeGuillou, *Electron. Lett.* **25**, 718 (1989).
- ³R. G. Wilson, R. N. Schwartz, C. R. Abernathy, S. J. Pearton, N. Newman, M. Rubin, T. Fu, and J. M. Zavada, *Appl. Phys. Lett.* **65**, 992 (1994).
- ⁴J. T. Torvik, R. J. Feuerstein, J. I. Pankove, C. H. Qiu, and F. Namavar, *Appl. Phys. Lett.* **69**, 2098 (1996).
- ⁵S. Kim, S. J. Rhee, D. A. Turnbull, E. E. Reuter, X. Li, J. J. Coleman, and S. G. Bishop, *Appl. Phys. Lett.* **71**, 231 (1997).
- ⁶D. M. Hansen, R. Zhang, N. R. Perkins, S. Safvi, L. Zhang, K. L. Bray, and T. F. Kuech, *Appl. Phys. Lett.* **72**, 1244 (1998).
- ⁷J. D. MacKenzie, C. R. Abernathy, S. J. Pearton, U. Hömmerich, J. T. Seo, R. G. Wilson, and J. M. Zavada, *Appl. Phys. Lett.* **72**, 2710 (1998).
- ⁸A. J. Steckl, M. Garter, R. Birkhahn, and J. Scofield, *Appl. Phys. Lett.* **73**, 2450 (1998).
- ⁹C. Ugolini, N. Nepal, J. Y. Lin, H. X. Jiang, and J. M. Zavada, *Appl. Phys. Lett.* **89**, 151903 (2006).
- ¹⁰R. Dahal, C. Ugolini, J. Y. Lin, H. X. Jiang, and J. M. Zavada, *Appl. Phys. Lett.* **93**, 033502 (2008).
- ¹¹C. Ugolini, N. Nepal, J. Y. Lin, H. X. Jiang, and J. M. Zavada, *Appl. Phys. Lett.* **90**, 051110 (2007).